7-29-2018

Full Field Computing for Elastic Pulse Dispersion in Inhomogeneous Bars

A. Berezovski
Tallinn University of Technology, arkadi.berezovski@cs.ioc.ee

R. Kolman
The Czech Academy of Sciences, kolman@it.cas.cz

M. Berezovski
Embry-Riddle Aeronautical University, berezovm@erau.edu

D. Gabriel
The Czech Academy of Sciences, gabriel@it.cas.cz

V. Adamek
New Technologies for the Information Society, vadamek@kme.zcu.cz

Full field computing for elastic pulse dispersion in inhomogeneous bars

A. Berezovski[1], R. Kolman[a,*], M. Berezovski[b], D. Gabriel[a], V. Adámek[c]

[a]*Institute of Thermomechanics, v.v.i., The Czech Academy of Sciences, Dolejškova 1402/5, 182 00 Praha 8, Czech Republic*
[b]*Department of Mathematics, Embry-Riddle Aeronautical University, 600 S. Clyde Morris Boulevard, Daytona Beach, Florida 32114-3990, USA*
[c]*NTIS - New Technologies for the Information Society, Faculty of Applied Sciences, University of West Bohemia, Technická 8, 301 00 Pilsen, Czech Republic*

Abstract

In the paper, the finite element method and the finite volume method are used in parallel for the simulation of a pulse propagation in periodically layered composites beyond the validity of homogenization methods. The direct numerical integration of a pulse propagation demonstrates dispersion effects and dynamic stress redistribution in physical space on example of a one-dimensional layered bar. Results of numerical simulations are compared with analytical solution constructed specifically for the considered problem. Analytical solution as well as numerical computations show the strong influence of the composition of constituents on the dispersion of a pulse in a heterogeneous bar and the equivalence of results obtained by two numerical methods.

Keywords: wave propagation, wave dispersion, heterogeneous solids, finite element method, finite volume method

1. Introduction

Wave propagation in a slender heterogeneous solid bar is the typical test problem for models of composite materials [1, 2, 3, 4, e.g.]. The modeling is

*Corresponding author
Email addresses: Arkadi.Berezovski@cs.ioc.ee (A. Berezovski), kolman@it.cas.cz (R. Kolman), mihhail.berezovski@erau.edu (M. Berezovski), gabriel@it.cas.cz (D. Gabriel), vadamek@kme.zcu.cz (V. Adámek)

necessary because macroscopic properties of composite materials are strongly influenced by the properties of their constituents. The macroscopic properties are usually determined by a homogenization, which yields the effective stresses and strains acting on the effective material.

The basic idea of homogenization consists in a replacement of a heterogeneous solid by a homogeneous one which, from the macroscopic point of view, behaves in the same way, as do its constituents, but with different, effective, values of the appropriate material constants [5]. This idea reappeared many times in the last two centuries, as it is indicated in recent reviews [5, 6, 7, 8]. Mathematical details of classical homogenization models can be found in [9].

Layered periodic materials represent the simplest possible pattern of composites from the theoretical point of view. Their modeling also has a rich history [10]. Constitutive models of effective properties for such materials are still under development using either ensemble averaging [11, 12], or integration over unit cell [13, 14], or scattering response [15]. However, as it is pointed out by Willis [16], "The broad conclusion is that an "effective medium" description of a composite medium provides a reasonable approximation for its response, so long as the predicted "effective wavelength" is larger than two periods of microstructure – say at least 2.5". This is confirmed recently on the example of Mindlin's microelasticity theory [17]. It is worth therefore to build tools for the analysis of interaction between layers and waves with shorter wavelength. The natural choice for such tools is provided by numerical methods due to their flexibility and universality. However, we need to be insured in the accuracy and stability of them. It is well known that numerical simulation of wave propagation even in a homogeneous solid bar under shock loading is under discussion so far both in the context of finite volume [18, 19] and finite element methods [20, 21, 22, 23]. This is why two different numerical methods – finite element method and finite volume method – are applied in the paper for the simulation of a pulse propagation in a slender heterogeneous solid bar. The pulse propagation is preferable from the practical point of view [24], while theoretically only the behavior of dispersion curves is of interest [25, 26, 27, e.g].

It should be repeated, following Zohdi [28] that "solutions to partial differential equations, of even linear material models, at infinitesimal strains, describing the response of small bodies containing a few heterogeneities are still open problems". Fortunately, the analytical solution is constructed specifically for the considered test problem by means of Laplace transform technique [29].

The objective of the paper is to demonstrate the influence of the composition of alternating layers on the dispersion of a short pulse and to compare results of simulation obtained by two different numerical methods with analytical solution of the problem.

In this paper, we consider propagation of a finite pulse, the length of which is comparable with the size of heterogeneities. The dispersion of the pulse is provided by the wave reflection and transmission in periodic layered structure where each layer is dispersionless. It is clearly demonstrated that strong dispersion effects depend not only on the size of heterogeneities but also on their mutual position.

2. Formulation of the problem

We consider wave propagation in a bar of constant cross section. The motion is assumed being one-dimensional and considered within the linear theory of elastodynamics [30, e.g]. It is governed by the balance of linear momentum, which in the absence of body forces has the form

$$\rho \frac{\partial v}{\partial t} - \frac{\partial \sigma}{\partial x} = 0, \tag{1}$$

where ρ is the matter density, v is the particle velocity, σ is the one-dimensional Cauchy stress. In the linear elasticity the Cauchy stress obeys the Hooke law $\sigma = E\,\varepsilon$, where E is the Young modulus and ε is the one-dimensional strain. . The wave speed in a bar is given for one-dimensional case by $c = \sqrt{E/\rho}$, therefore, the Hooke law has the following form

$$\sigma = \rho c^2\,\varepsilon. \tag{2}$$

The strain and velocity are related by the compatibility condition

$$\frac{\partial \varepsilon}{\partial t} = \frac{\partial v}{\partial x}. \tag{3}$$

In terms of the displacement, the balance of linear momentum is represented in the form of the wave equation

$$\frac{\partial^2 u}{\partial t^2} = c^2 \frac{\partial^2 u}{\partial x^2}, \tag{4}$$

since the displacement u is connected to the strain and particle velocity by

$$v = \frac{\partial u}{\partial t}, \quad \varepsilon = \frac{\partial u}{\partial x}. \tag{5}$$

It should be noted that the material parameters ρ and c are distinct in different parts of the bar. However, they keep constant values for each computational cell in numerical methods for the bar with piecewise constant distribution of material parameters such as Young modulus and matter density.

It is assumed that the bar is occupied the interval $0 \leq x \leq L$. Initially, the bar is at rest. The left end of the bar is loaded by the pulse, the shape of which is formed by an excitation of the stress for a limited time period (Fig. 1). Then the stress at the left end is zero. The right end of the bar is fixed.

Figure 1: A scheme of the test problem - a pulse loaded free-fixed bar

For convenience, the bar is divided into three parts. The left and the right parts of the bar are supposed to be homogeneous and made from the same stiff material. The central part of the bar contains inhomogeneity provided by inclusions of a more soft materials (see Fig. 2). The solution of system of equations (1) – (3) or equation (4) satisfying formulated initial and boundary conditions is obtained by means of analytical and numerical methods in the following sections.

3. Analytical solution

To verify the correctness and the accuracy of numerical results presented in Section 4, the analytical solution of the above described problem was derived. The main idea of the analytical procedure is based on the fact that the final solution for a bar with piecewise constant distribution of material properties can be constructed from the solutions derived for each of homogeneous parts of the bar combined through the boundary conditions formulated at their interfaces.

It is clear that the propagation of longitudinal waves in arbitrary ith homogeneous part is formally described by the same equation as (4). The solution for such particular problem with general boundary conditions can be simply derived based on the solution presented in [30]. Applying the Laplace

transform in time [29] to (4) with zero initial conditions one obtains a simple ODE the solution of which can be written as

$$\bar{u}_i(x_i, p) = C_{1,i}(p) \sinh\left(\frac{px_i}{c_i}\right) + C_{2,i}(p) \cosh\left(\frac{px_i}{c_i}\right), \tag{6}$$

where p is a complex number. The variable x_i in (6) represents a local coordinate defined for the ith part of the bar, the constant c_i is the wave speed in this part and the function $\bar{u}_i(x_i, p)$ denotes the Laplace transform of the corresponding displacement $u_i(x_i, t)$. The unknown complex functions $C_{1,i}$ and $C_{2,i}$ can then be determined through the boundary conditions of the problem and through the conditions of displacement and stress continuity formulated for each interface between two parts with different material properties. It leads to a system of algebraic equations in complex domain. Substituting its solution into (6) one obtains the final solution of the problem in Laplace domain.

The last step of the analytical procedure consists in the inversion of previously mentioned formulas back to time domain. It can be done analytically by means of the residue theorem in this case or numerically by using a suitable algorithm. Given the low computational demands and the versatility, the latter approach was used in this work. In particular, an algorithm based of FFT and Wynn's epsilon accelerator was applied to manage the inverse Laplace transform problem. As proved in [29], this algorithm is effective and robust and it gives very precise results for various problems of elastodynamics. The analytical results for specific study cases are presented together with the numerical solutions in Section 5.

4. Numerical procedures

Application of numerical methods suggests a discretization in space and time. For this purpose, the interval $0 \leq x \leq L$ is divided into N elements of the same size. The state of each element is described differently in distinct methods. In this paper, we compare results obtained by the finite element method (FEM) and the finite volume method (FVM) in case of explicit approaches of these methods.

4.1. Finite element method and explicit time integration

In this section, we shortly remind the basic of the finite element method in the one-dimensional case for linear elastodynamics. Spatial discretization

of elastodynamics problems by the finite element method leads to the matrix form [31]

$$\mathbf{M}\ddot{\mathbf{d}}(t) + \mathbf{K}\mathbf{d}(t) = \mathbf{F}(t), \quad t \in [0, T], \tag{7}$$

$$\mathbf{d}(0) = \mathbf{d}_0, \tag{8}$$

$$\dot{\mathbf{d}}(0) = \dot{\mathbf{d}}_0. \tag{9}$$

Here $\mathbf{M}$ denotes the mass matrix, $\mathbf{K}$ marks the stiffness matrix, $\mathbf{F}$ is the time-dependent load vector, $\mathbf{d}$, $\dot{\mathbf{d}}$ and $\ddot{\mathbf{d}}$ contain nodal variables, namely, displacements, velocities, and accelerations, respectively, t is the time and dots denote time derivatives. Initial values for displacements and velocities are denoted by $\mathbf{d}_0$ and $\dot{\mathbf{d}}_0$. The initial acceleration vector should satisfy the equation of motion at the time t_0: $\mathbf{M}\ddot{\mathbf{d}}_0 + \mathbf{K}\mathbf{d}_0 = \mathbf{F}_0$.

Practically, the stiffness matrix $\mathbf{K}$ and the mass matrix $\mathbf{M}$ are defined by the relationships

$$\mathbf{K} = \int_\Omega \mathbf{B}^{\mathrm{T}} E \mathbf{B} \, \mathrm{d}\Omega, \qquad \mathbf{M} = \int_\Omega \rho \mathbf{N}^{\mathrm{T}} \mathbf{N} \, \mathrm{d}\Omega, \tag{10}$$

and the right hand side is given

$$\mathbf{F} = \int_{\Gamma_N} \mathbf{N}^{\mathrm{T}} h \, \mathrm{d}\Gamma - \int_\Omega \mathbf{B}^{\mathrm{T}} E \mathbf{B} g \, \mathrm{d}\Omega - \int_\Omega \rho \ddot{g} \mathbf{N}^{\mathrm{T}} \mathbf{N} \, \mathrm{d}\Omega, \tag{11}$$

where $\mathbf{B}$ is the strain-displacement matrix, $\mathbf{N}$ stores the displacement shape functions, h is the traction prescribed on boundary Γ_N, g is the displacement prescribed as the Dirichlet boundary condition.

In this paper, we assume linear shape functions and diagonal mass matrix obtained by row-summing of the consistent mass matrix given by (10). The mass matrix, $\mathbf{M}$, and the stiffness matrix, $\mathbf{K}$, are evaluated by the Gauss-Legendre quadrature formula [31].

For time integration, we use the central difference method [31] which is based on the approximate relationships between the nodal displacements $\mathbf{d}$, velocities $\mathbf{v}$ and accelerations $\mathbf{a}$ so that

$$\mathbf{v}^k = \frac{1}{2\Delta t} \left(\mathbf{d}^{k+1} - \mathbf{d}^{k-1} \right), \tag{12}$$

$$\mathbf{a}^k = \frac{1}{(\Delta t)^2} \left(\mathbf{d}^{k+1} - 2\mathbf{d}^k + \mathbf{d}^{k-1} \right). \tag{13}$$

Here the superscript k denotes the time level and Δt is the time step size. Substituting relationships (12) and (13) into equations of motion (7) at time t, we get a system of algebraic equations which we can solve for displacements at the next time step $t + \Delta t$

$$\mathbf{M}\mathbf{d}_{n+1} = \mathbf{F}_n(\Delta t)^2 - \left(\mathbf{K}(\Delta t)^2 - 2\mathbf{M}\right)\mathbf{d}_n - \mathbf{M}\mathbf{d}_{n-1}. \tag{14}$$

Stress field $\sigma(x, t_{n+1})$ is computed from the approximated displacement field given by $\mathbf{d}_{n+1}$.

This explicit method is only conditionally stable. The critical time step Δt_{cr} securing the stability of the central difference method for a linear undamped system is $\Delta t_{cr} = 2/\omega_{max}$ [32], where ω_{max} being the maximum eigenfrequency related to the maximum eigenvalue λ_{max} of the generalized eigenvalue problem $\mathbf{K}\mathbf{u} = \lambda\mathbf{M}\mathbf{u}$ by $\omega^2 = \lambda$. In the one-dimensional case with a structured mesh in a homogeneous material, Δt_{cr} is exactly given by $\Delta t_{cr} = h/c$, where h is the finite element size and c is the wave speed in an elastic bar. The time integration by the critical time step produces results without numerical dispersion in 1D case, see [33].

4.2. Finite volume method

In this section, we shortly introduce the finite volume scheme based on the approach presented in [34]. In finite volume methods, the fields of interest (stress and velocity fields) are uniform inside each element [35]. This means that shape functions are piecewise constant. Though this is not a good approximation, it can be interpreted in terms of thermodynamic systems [36]. Since we cannot expect that this thermodynamic system is in equilibrium, its local equilibrium state is described by averaged values of field quantities. Therefore, so-called excess quantities are introduced in the spirit of the thermodynamics of discrete systems

$$\sigma = \bar{\sigma} + \Sigma, \qquad v = \bar{v} + \mathcal{V}. \tag{15}$$

Here overbars denote averaged quantity and Σ and $\mathcal{V}$ are the corresponding excess quantities. Excess quantities represent the difference between the values of entire and averaged fields.

Integrating the balance of linear momentum (1) over the computational cell under assumption of constant material parameters (Young modulus, matter density) per cell we have

$$\rho\frac{\partial}{\partial t}\int_{x_n}^{x_{n+1}} v dx = \sigma_n^+ - \sigma_n^- = \overline{\sigma}_n + \Sigma_n^+ - \overline{\sigma}_n - \Sigma_n^- = \Sigma_n^+ - \Sigma_n^-, \tag{16}$$

where superscripts "+" and "-" denote values of the quantities at right and left boundaries of the cell, respectively. The corresponding integration of the kinematic compatibility (3) results in

$$\frac{\partial}{\partial t}\int_{x_n}^{x_{n+1}} \varepsilon dx = v_n^+ - v_n^- = \overline{v}_n + \mathcal{V}_n^+ - \overline{v}_n - \mathcal{V}_n^- = \mathcal{V}_n^+ - \mathcal{V}_n^-. \qquad (17)$$

Averaged quantities a defined as follows:

$$\overline{v}_n = \frac{1}{\Delta x}\int_{x_n}^{x_{n+1}} v(x,t_k)dx, \quad \overline{\varepsilon}_n = \frac{1}{\Delta x}\int_{x_n}^{x_{n+1}} \varepsilon(x,t_k)dx. \qquad (18)$$

Standard approximation of time derivatives in (16) and (17) allows us to write a first-order Godunov-type scheme in terms of averaged and excess quantities

$$(\rho\overline{v})_n^{k+1} - (\rho\overline{v})_n^k = \frac{\Delta t}{\Delta x}\left(\Sigma_n^+ - \Sigma_n^-\right), \qquad (19)$$

$$\bar{\varepsilon}_n^{k+1} - \bar{\varepsilon}_n^k = \frac{\Delta t}{\Delta x}\left(\mathcal{V}_n^+ - \mathcal{V}_n^-\right). \qquad (20)$$

Here the superscript k denotes time step and the subscript n denotes the number of computational cell.

Though excess quantities are determined formally everywhere inside elements, we need to know only their values at the boundaries of the elements, where they describe the interactions between neighboring elements. The values of excess quantities at the boundaries (numerical fluxes) are determined by the continuity of entire fields

$$(\bar{\sigma})_{n-1} + (\Sigma^+)_{n-1} = (\bar{\sigma})_n + (\Sigma^-)_n, \qquad (21)$$

$$(\bar{v})_{n-1} + (\mathcal{V}^+)_{n-1} = (\bar{v})_n + (\mathcal{V}^-)_n, \qquad (22)$$

and the conservation of the Riemann invariants [36]

$$\rho_n c_n \mathcal{V}_n^- + \Sigma_n^- = 0, \qquad (23)$$

$$\rho_{n-1} c_{n-1} \mathcal{V}_{n-1}^+ - \Sigma_{n-1}^+ = 0. \qquad (24)$$

The obtained system of linear equations for excess quantities (21) – (24) is solved exactly. Having the values of numerical fluxes, we can update the state of each element for the next time step by means of numerical scheme (19) – (20). The described procedure is in fact the conservative wave-propagation

algorithm [34]. As the result, the reflection and transmission of waves at each interface are handled automatically. The scheme is explicit and solved without a matrix solver. The mentioned scheme is conditionally stable for the time step size Δt satisfying the stability condition in the form $\Delta t \leq \Delta x/c$, where Δx is the grid size.

In both mentioned explicit computational methods for wave propagation in heterogeneous bars, we choose the time step size as $\Delta t = \min(\Delta x_{cell}/c_{0\,cell})$ over all cells.

5. Results of numerical simulations

In this section, we compare several results of simulations of wave propagation in heterogeneous bars with corresponding analytical solutions.

5.1. Two-phase layered composite

We start with the simulation of a pulse propagation in the so-called two-phase layered composite following the terminology introduced in [14]. This means that the heterogeneity is composed by alternating layers of two different materials. The properties of the matrix material for the test problem are chosen artificially. In the dimensionless setting they are the following: $\rho_1 = 1, c_1 = 1$, with corresponding $E_1 = c_1^2\rho_1 = 1$. Accordingly, the dimensionless properties of embedded layers are: $\rho_2 = 0.6, c_2 = 0.96$, with $E_2 = 0.55296$. The computational domain is divided into 1500 elements of the same size. Choosing the dimensionless length of the bar equal to 1, we have for the size of an space step $\Delta x = 1/1500$. The choice of the time step is indicated at the end of the previous section. The thickness of each layer is equal to 90 space elements. The alternating layers are placed starting from 300th space step until 1200th space step (Fig. 2). We focus on propagation

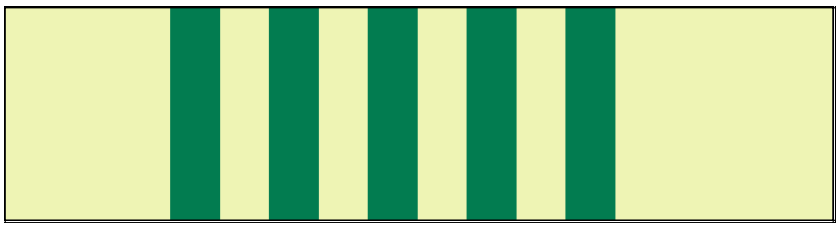

Figure 2: Distribution of thick periodic layers. Yellow domain corresponds to material 1, green domain - to material 2.

of a pulse with finite time duration. Initial pulse is formed by the excitation of stress at the left end of the bar

$$F(t) = \sigma(0,t) = \frac{1}{2}(1+\cos(\pi(t-20)/20)). \tag{25}$$

The time duration of the initial pulse is set with respect to size of layers and wave speed in layers. The length of the initial pulse is shorter than the size of layers in this case. Its shape is shown in Fig. 3. Its frequency spectrum is

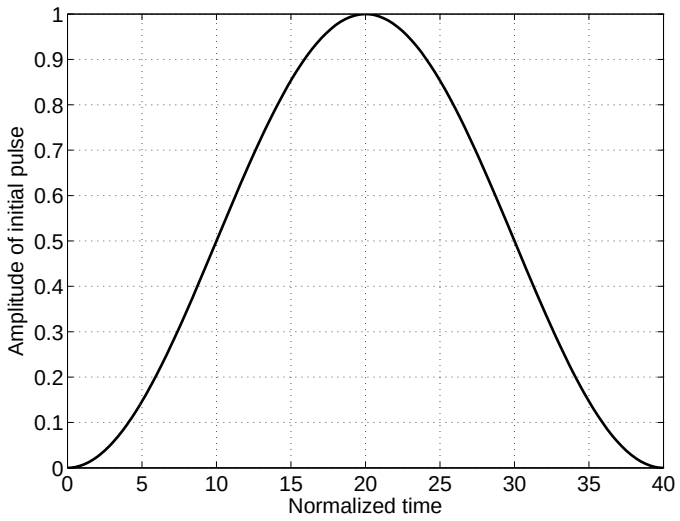

Figure 3: Initial pulse shape

given in the next figure with a zooming of small frequencies area.

Fig. 5 shows the evolution of the initial pulse in time due to interaction with layers of different materials. In this Fig., vertical lines display the boundaries of distinct layers and arrows indicate the direction of propagation of the main pulse.

Now we compare results of numerical simulations with the analytical solution of the pulse propagation problem. We start with FEM simulation. The distribution of the stress at 1400th time step computed by FEM is shown in Fig. 6 together with the initial pulse recorded at 200th time step. As one can see, there is practically no difference in the results computed by FEM and obtained analytically.

Similar great agreement between numerical and analytical results have been obtained also in the case of FVM. The corresponding comparison with

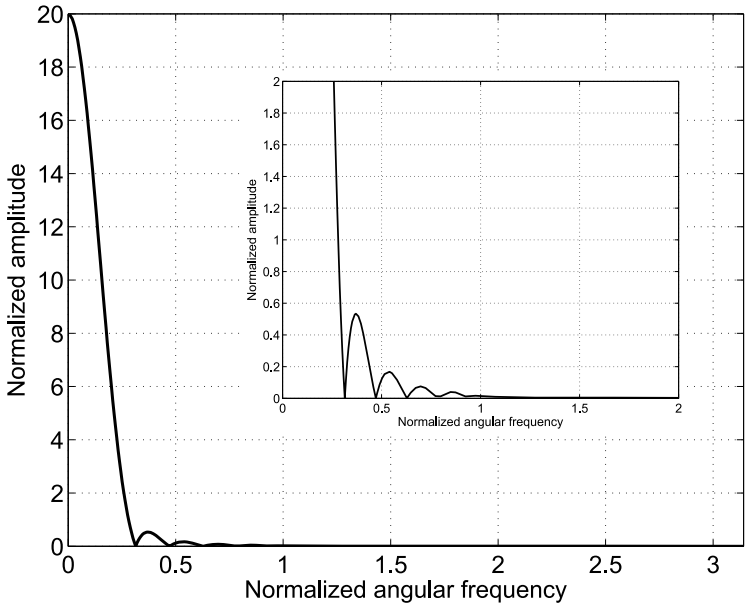

Figure 4: Frequency spectrum of the initial pulse

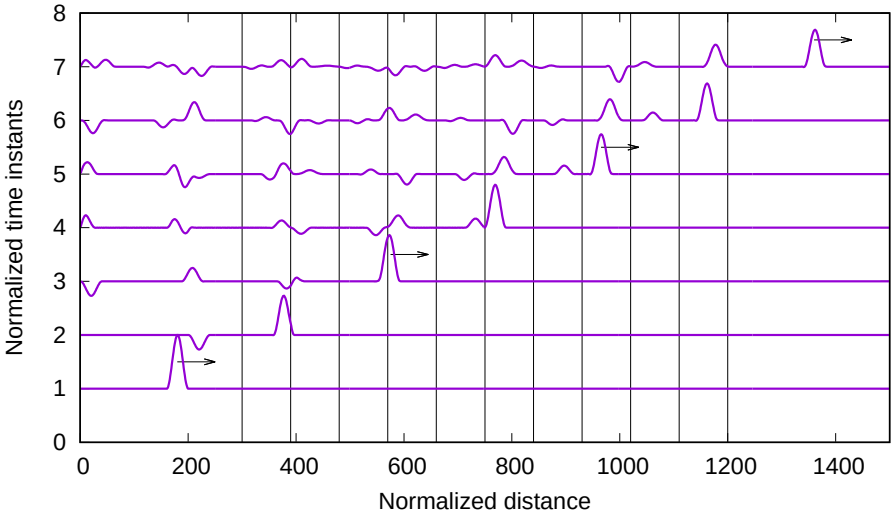

Figure 5: Stress distribution at distinct time instants

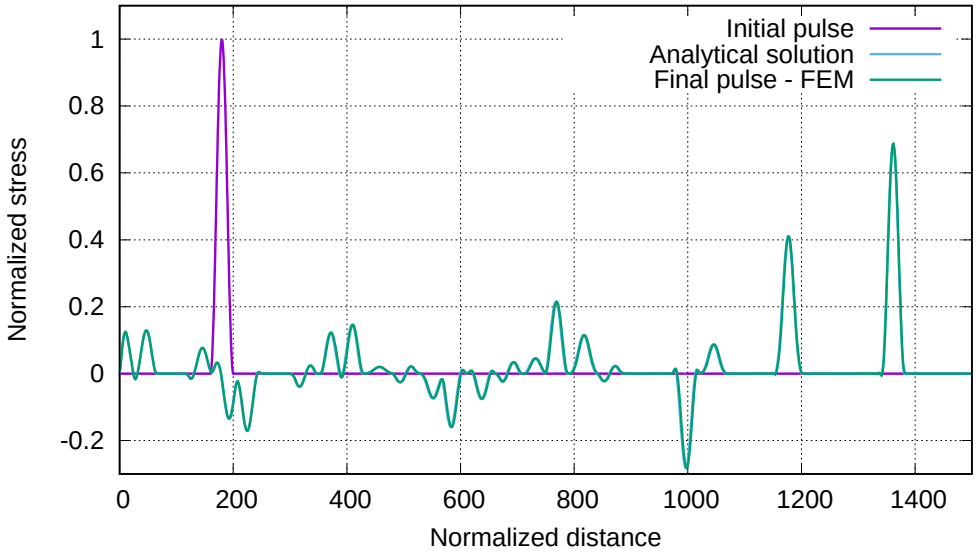

Figure 6: Stress distribution along the bar at 1400th time step in the case of thick periodic layers

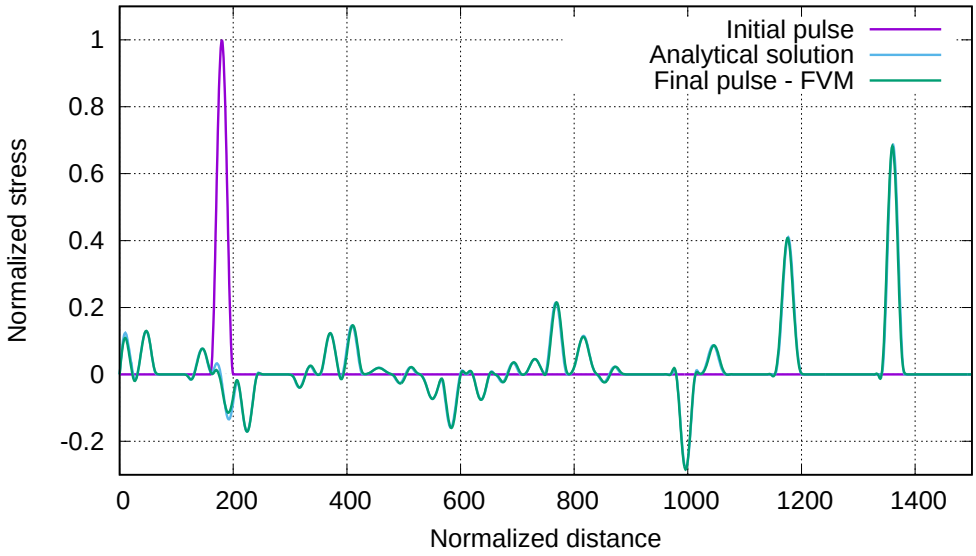

Figure 7: Stress distribution along the bar at 1400th time step in the case of thick periodic layers

the analytical solution is presented in Fig. 7. A small distinction in the distribution of the stress close to the left end of the bar is due to a different handling of stress-free conditions in FEM and FVM.

It is clearly visible that in addition to many reflections, two main transmitted stress pulses are formed by the periodic heterogeneity. This demonstrates a strong dispersion provided by the alternating layers. In the considered case, the amplitude of the leading pulse is greater than the amplitude of the following one.

Now we turn to more thin alternating layers to study the influence of the size of the heterogeneity. We apply the same loading as previously, but the thickness of each layer is reduced to 30 space elements. In this case the length of the initial pulse is greater than the size of layers. The periodic heterogeneity is placed in the same position as previously, as it can be seen in Fig. 8.

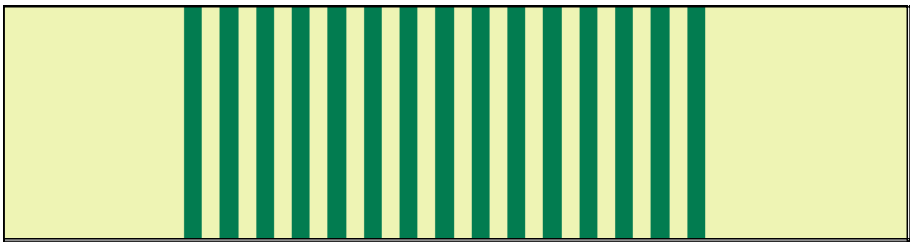

Figure 8: Distribution of thin periodic layers

The comparison of analytical solution and results of computations by FEM is presented in Fig. 9. As in the previous case, results of computations by FEM coincide with analytical predictions. Calculations performed by means of FVM (Fig. 10) shows small differences from analytical solution in the vicinity of the left end of the bar. This confirms once more the equivalence of finite element and finite volume methods for smooth solutions, as it is pointed out by Idelsohn and Oñate [37]. In contrast to the case of thick layers, here the leading transmitted pulse is smaller in amplitude than the following one. The difference in the shape and position of transmitted pulses for thick and thin alternating layers indicates a strong influence of the size of the heterogeneity on the wave dispersion.

It is clear that there exists an infinite number of relations between the length of the pulse and the size of heterogeneity in layered materials, which are beyond the validity of homogenization methods. As it is shown, all such

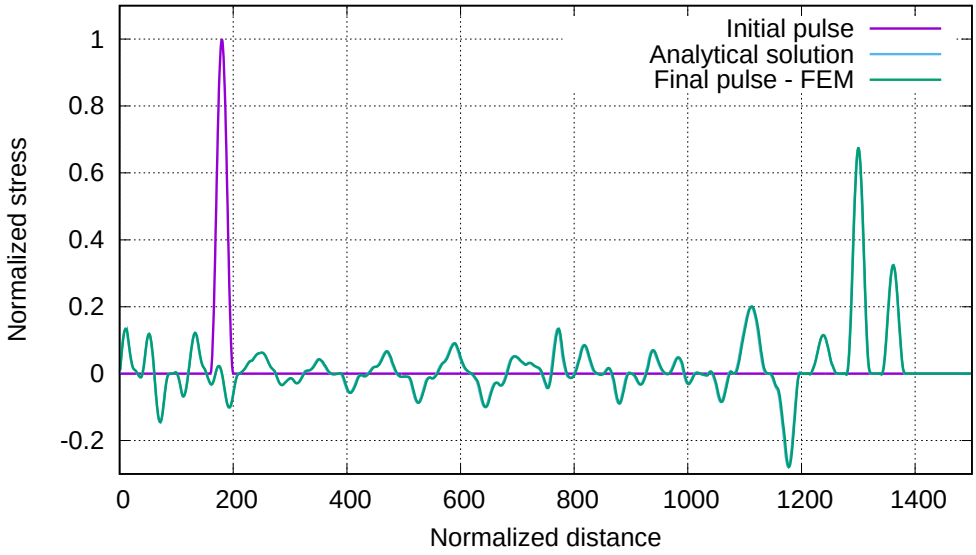

Figure 9: Stress distribution along the bar at 1400th time step in the case of thin periodic layers

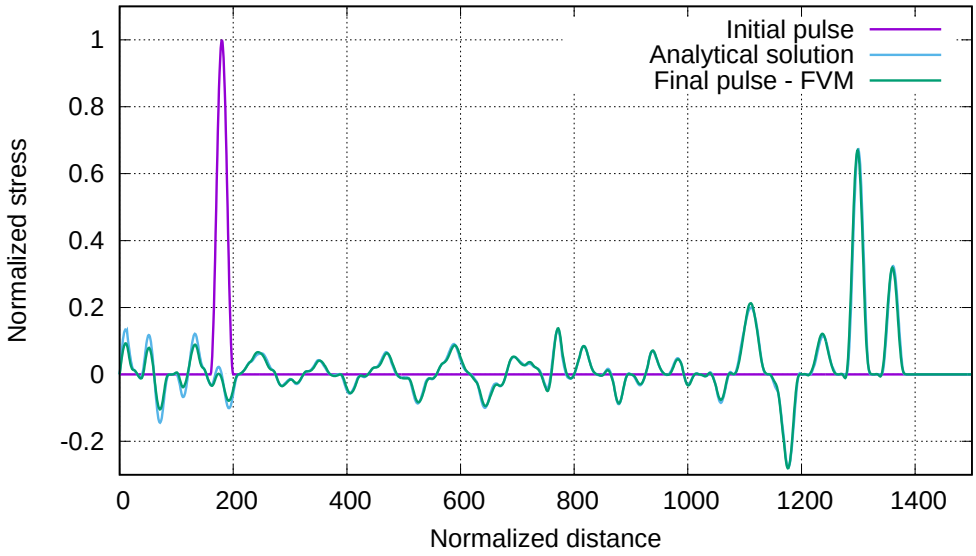

Figure 10: Stress distribution along the bar at 1400th time step in the case of thin periodic layers

cases can be computed precisely by means of accurate numerical methods.

5.2. Three-phase layered composite

To illustrate the capabilities of numerical simulations, we consider the so-called three-phase periodic composite. Considering first a symmetric composition, we assume that each thick layer presented in the previous section is divided into three identical parts, and the central part of each thick layer is occupied with the material of properties, which are intermediate between the properties of hard and soft materials (Fig. 11).

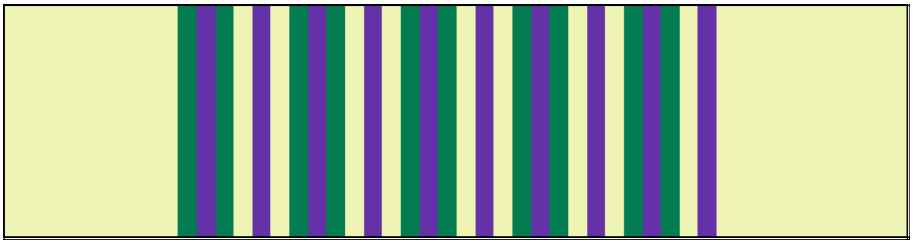

Figure 11: Symmetric distribution of three-phase periodic layers. Violet color indicates material 3.

Namely, we apply dimensionless values $\rho_3 = 0.8, c_3 = 0.98$, $E_3 = 0.76832$ for the third material marked by the violet color in Fig. 11. The initial and boundary conditions are the same as in the previous cases. Analytical solution and numerical simulations demonstrate again the strong dispersion manifested in the transformation of the initial pulse into two main transmitted pulses with almost equal amplitudes (Fig.12).

Now we change the arrangement of the layers keeping the volume fractions of the layers unchanged. We assume that the layer with intermediate properties is moved into the beginning of each thick layer. The resulting new composition is shown in Fig. 13. Analytical solution as well as numerical simulations of the wave propagation under the same loading as in the previous case show a completely different evolution of the stress pulse: only a single transmitted pulse is formed after the heterogeneous zone. Due to the dispersion, the amplitude of the transmitted pulse is decreased in comparison with the initial pulse.

Of course, there is infinitely many possible arrangements of distinct layers in composites. Each of them produces a specific shape of the transmitted signal. As it is demonstrated, accurate numerical methods are capable to

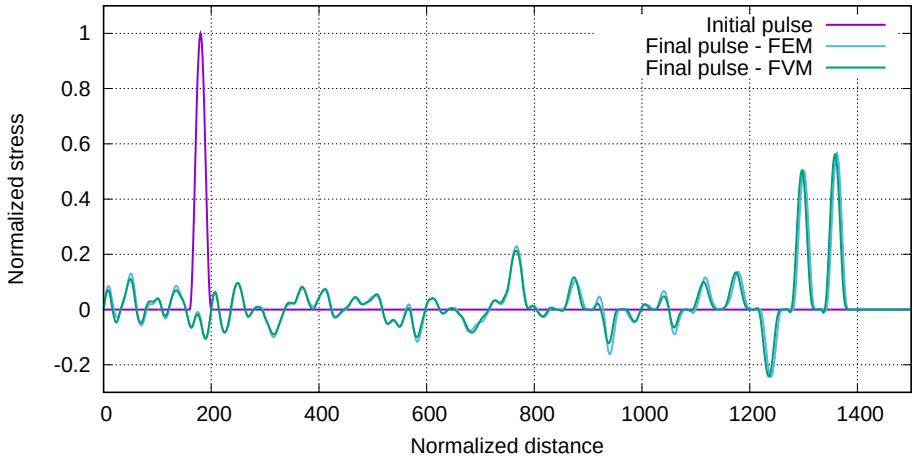

Figure 12: Stress distribution along the bar at 1400th time step in the case of three-phase symmetric periodic layers. FEM results coincide with analytical solution

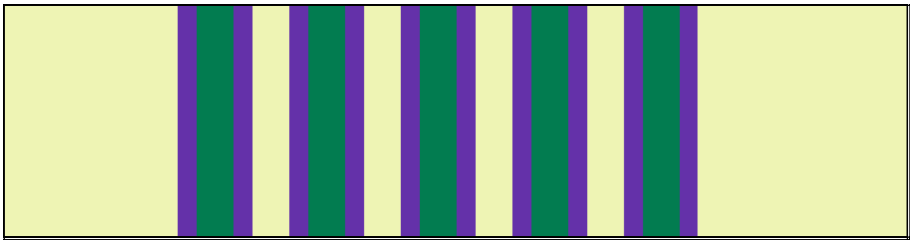

Figure 13: Another distribution of three-phase periodic layers

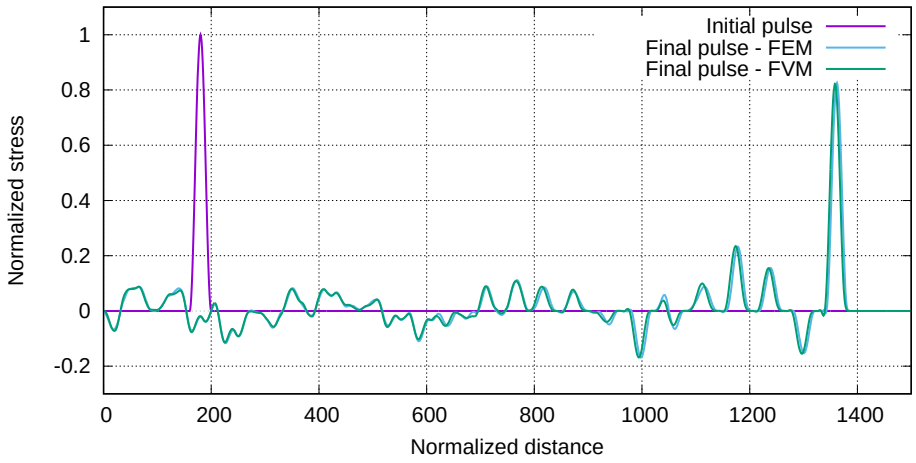

Figure 14: Stress distribution along the bar at 1400th time step in the case of another arrangement of three-phase symmetric periodic layers. FEM results coincide with analytical solution

predict any possible wave field in layered composites (at least in the one-dimensional case). Additional examples of one-dimensional wave dispersion in layered composites can be found in [38]. It is worth to note that the change of material properties of the layers also affects the wave dispersion. This extends the area of possible applications but does not restrict the capabilities of the applied numerical methods.

6. Conclusions

Composite materials are broadly applied in industry because of their excellent designable characteristics. To meet a desired functionality, the microstructure in a composite material can be architectured. The recent advancement in additive manufacturing eased the fabrication of complex structures with a very wide range of materials.

Dispersion is a characteristic feature of composites. It manifests itself in the change of the shape and/or of the length of a signal during its propagation through composites or heterogeneous structures. For harmonic waves, dispersion is expressed in the relation between frequency and wave number. While it may be sufficient from the theoretical point of view, it is also helpful to observe directly the transformation of a signal due to heterogeneity in a

material. This is why two different numerical methods – FEM and FVM – are used for the simulation of a pulse propagation in periodically layered composites beyond the validity of homogenization methods. The results of simulations of one-dimensional pulse propagation by the two numerical approaches are compared with analytical solution and practically coincide in all considered cases. This coincidence with analytical solution ensures the accuracy of the results obtained numerically. As it is shown, even a simple rearrangement of the position of layers provides the possibility of manipulation of the shape of a transmitted pulse. Though this result can be qualitatively expected in advance, it is not easy to predict the shape of the final pulse quantitatively.

Accurate numerical computation of the full-field solution for pulse propagation in layered materials allows to analyze the influence of heterogeneity beyond the possibilities of homogenization methods. The difference in the transmitted signals due to a simple change of the positions of the same layers, which is invisible from the point of view of homogenized effective media, is demonstrated clearly.

The full scale direct simulation of wave dispersion in composites has become increasingly feasible with advanced numerical techniques and rapidly enhanced computing power. A major advantage of numerical simulation is its generality, capable of predicting accurate wave fields for any composite with arbitrarily distributed layers of different sizes.

In future work, we will focus on modelling of elastic wave propagation in two- and three-dimensional specimens composed by heterogeneous and anisotropic materials with a special attention on Rayleigh-edge waves [39] and wave propagation in metamaterials [40] and piezomaterials [41].

Acknowledgements

The work of A. Berezovski and D. Gabriel was supported by the Centre of Excellence for Nonlinear Dynamic Behaviour of Advanced Materials in Engineering CZ.02.1.01/0.0/0.0/15_003/0000493 (Excellent Research Teams) in the framework of Operational Programme Research, Development and Education. The work of R. Kolman was supported by the grant projects with No. 17-22615S and 17-12925S of the Czech Science Foundation (CSF) within institutional support RVO:61388998. The work of V. Adámek was supported by the project LO1506 of the Czech Ministry of Education, Youth and Sports. Further, the work has been supported by the bilateral project between the Estonian Academy of Sciences and the Czech Academy of Sciences (project

No. ETA-15-03 entitled 'Advanced numerical modelling of dynamic processes in solids').

[1] B. Clements, J. Johnson, R. Hixson, Stress waves in composite materials, Physical Review E 54 (6) (1996) 6876–6888.

[2] A. Chakraborty, S. Gopalakrishnan, Various numerical techniques for analysis of longitudinal wave propagation in inhomogeneous one-dimensional waveguides, Acta Mechanica 162 (1-4) (2003) 1–27.

[3] M. I. Hussein, G. M. Hulbert, R. A. Scott, Dispersive elastodynamics of 1d banded materials and structures: design, Journal of Sound and Vibration 307 (3) (2007) 865–893.

[4] T. Hui, C. Oskay, A high order homogenization model for transient dynamics of heterogeneous media including micro-inertia effects, Computer Methods in Applied Mechanics and Engineering 273 (2014) 181–203.

[5] K. Z. Markov, Elementary micromechanics of heterogeneous media, in: Heterogeneous Media, Springer, 2000, pp. 1–162.

[6] P. Kanouté, D. Boso, J. Chaboche, B. Schrefler, Multiscale methods for composites: a review, Archives of Computational Methods in Engineering 16 (1) (2009) 31–75.

[7] C. T. Herakovich, Mechanics of composites: a historical review, Mechanics Research Communications 41 (2012) 1–20.

[8] H. Reda, K. Elnady, J. Ganghoffer, H. Lakiss, Wave propagation in pre-deformed periodic network materials based on large strains homogenization, Composite Structures 184 (Supplement C) (2018) 860 – 871.

[9] J. Aboudi, Mechanics of Composite Materials: A Unified Micromechanical Approach, Elsevier, 1991.

[10] L. Brillouin, Wave Propagation in Periodic Structures: Electric Filters and Crystal Lattices, McGraw-Hill Book Company, 1946.

[11] J. Willis, Exact effective relations for dynamics of a laminated body, Mechanics of Materials 41 (4) (2009) 385–393.

[12] J. R. Willis, The construction of effective relations for waves in a composite, Comptes Rendus Mécanique 340 (4-5) (2012) 181–192.

[13] S. Nemat-Nasser, A. Srivastava, Overall dynamic constitutive relations of layered elastic composites, Journal of the Mechanics and Physics of Solids 59 (10) (2011) 1953–1965.

[14] A. Srivastava, S. Nemat-Nasser, On the limit and applicability of dynamic homogenization, Wave Motion 51 (7) (2014) 1045–1054.

[15] A. V. Amirkhizi, Homogenization of layered media based on scattering response and field integration, Mechanics of Materials 114 (2017) 76–87.

[16] J. Willis, Some thoughts on dynamic effective properties—a working document, arXiv preprint arXiv:1311.3875.

[17] A. Berezovski, On the Mindlin microelasticity in one dimension, Mechanics Research Communications 77 (2016) 60–64.

[18] B. Boutin, C. Chalons, F. Lagoutiere, P. LeFloch, A sharp interface and fully conservative scheme for computing nonclassical shocks, in: Numerical Mathematics and Advanced Applications, Springer, 2008, pp. 217–224.

[19] D. I. Ketcheson, M. Parsani, R. J. LeVeque, High-order wave propagation algorithms for hyperbolic systems, SIAM Journal on Scientific Computing 35 (1) (2013) A351–A377.

[20] K. Park, S. Lim, H. Huh, A method for computation of discontinuous wave propagation in heterogeneous solids: Basic algorithm description and application to one-dimensional problems, International Journal for Numerical Methods in Engineering 91 (6) (2012) 622–643.

[21] A. Idesman, D. Pham, J. Foley, M. Schmidt, Accurate solutions of wave propagation problems under impact loading by the standard, spectral and isogeometric high-order finite elements. Comparative study of accuracy of different space-discretization techniques, Finite Elements in Analysis and Design 88 (2014) 67–89.

[22] R. Kolman, S. S. Cho, K. C. Park, Efficient implementation of an explicit partitioned shear and longitudinal wave propagation algorithm, International Journal for Numerical Methods in Engineering 107 (7) (2016) 543–579, nme.5174.

[23] R. Kolman, M. Okrouhlík, A. Berezovski, D. Gabriel, J. Kopačka, J. Plešek, B-spline based finite element method in one-dimensional discontinuous elastic wave propagation, Applied Mathematical Modelling 46 (2017) 382–395.

[24] M. Dona, M. Lombardo, G. Barone, Experimental study of wave propagation in heterogeneous materials, in: Proceedings of the Fifteenth International Conference on Civil, Structural and Environmental Engineering Computing, Prague, 1-4 Sept. 2015, © Civil-Comp Limited, 2015.

[25] C.-T. Sun, J. D. Achenbach, G. Herrmann, Continuum theory for a laminated medium, Journal of Applied Mechanics 35 (3) (1968) 467–475.

[26] A. N. Norris, Waves in periodically layered media: A comparison of two theories, SIAM Journal on Applied Mathematics 53 (5) (1993) 1195–1209.

[27] G. Carta, M. Brun, A dispersive homogenization model based on lattice approximation for the prediction of wave motion in laminates, Journal of Applied Mechanics 79 (2) (2012) 021019.

[28] T. I. Zohdi, P. Wriggers, An Introduction to Computational Micromechanics, Springer Science & Business Media, 2008.

[29] V. Adámek, F. Valeš, J. Červ, Numerical Laplace inversion in problems of elastodynamics: Comparison of four algorithms, Advances in Engineering Software 113 (2017) 120 – 129.

[30] K. F. Graff, Wave Motion in Elastic Solids, Clarendon Press, 1975.

[31] T. Hughes, The Finite Element Method: Linear Static and Dynamic Finite Element Analysis, Dover Civil and Mechanical Engineering, Dover Publications, 2000.

[32] K. Park, Practical aspects of numerical time integration, Computers & Structures 7 (3) (1977) 343 – 353.

[33] R. Kolman, J. Plešek, J. Červ, M. Okrouhlík, P. Pařík, Temporal-spatial dispersion and stability analysis of finite element method in explicit elastodynamics, International Journal for Numerical Methods in Engineering 106 (2) (2016) 113–128, nme.5010.

[34] A. Berezovski, J. Engelbrecht, G. A. Maugin, Numerical Simulation of Waves and Fronts in Inhomogeneous Solids, World Scientific, 2008.

[35] T. Barth, M. Ohlberger, Finite volume methods: Foundation and analysis, in: Encyclopedia of Computational Mechanics, Volume 1, Fundamentals, 2004, pp. 439–474.

[36] A. Berezovski, Thermodynamic interpretation of finite volume algorithms, Journal of Structural Mechanics (Rakenteiden Mekaniikka) 44 (2011) 156–171.

[37] S. R. Idelsohn, E. Oñate, Finite volumes and finite elements: Two 'good friends', International Journal for Numerical Methods in Engineering 37 (19) (1994) 3323–3341.

[38] M. Berezovski, A. Berezovski, T. Soomere, B. Viikmäe, On wave propagation in laminates with two substructures, Estonian Journal of Engineering 16 (3) (2010) 228–242.

[39] J. Cerv, T. Kroupa, J. Trnka, Influence of principal material directions of thin orthotropic structures on Rayleigh-edge wave velocity, Composite Structures 92 (2) (2010) 568 – 577.

[40] H. Reda, Y. Rahali, J. Ganghoffer, H. Lakiss, Wave propagation in 3D viscoelastic auxetic and textile materials by homogenized continuum micropolar models, Composite Structures 141 (Supplement C) (2016) 328 – 345.

[41] Y. Zhou, C. L, W. Chen, Bulk wave propagation in layered piezomagnetic/piezoelectric plates with initial stresses or interface imperfections, Composite Structures 94 (9) (2012) 2736 – 2745.